Poster

Chemodynamics of Blue Compact Dwarf galaxies

F. Campuzano-Castro[1,2], G. F. Hägele[1,2], G. Bosch[1,2], V. Firpo[3,4],
N. Morrell[5], M. Cardaci[1,2]

[1]*Facultad de Ciencias Astronómicas y Geofísicas, Universidad Nacional de La Plata (FCAG-UNLP)*
[2]*Instituto de Astrofísica de La Plata (IALP-CONICET)*
[3]*Universidad de La Serena*
[4]*Gemini Observatory, Chile*
[5]*Las Campanas Observatory, Chile*

Abstract. This work presents a brief summary of the analysis we are performing on the physical and chemical properties of the ionizing gas in star-forming regions belonging to two Blue Compact Dwarf galaxies (BCDs), using high resolution echelle spectra. Our aim is to perform a detailed study of the Chemodynamics on BCDs. To do that, we use our own Python code using the LMFIT (Non-Linear Least-Squares Minimization and Curve-Fitting for Python) package. We deconvolve the emission-line profiles fitting several gaussians to the different kinematical components to be able to estimate the properties and the nature of the ionized gas. Our next step is to use the kinematical information to perform the chemical abundance analysis and to infer the physical properties of the gas (the chemodynamical study) by using the methodology published in Hägele et al. (2008, 2012).

1. Introduction

Giant Extragalactic Hɪɪ Regions (GHɪɪRs) are extended objects, very luminous and located in the discs of spirals and in irregular galaxies. They are formed due to the presence of young and massive stars whose strong ultraviolet flux ionizes their surrounding gas. The observed emission line spectra of Hɪɪ galaxies and Blue Compact Dwarf galaxies (BCDs) are similar to those shown by Giant Hɪɪ Regions (Sargent & Searle, 1970; French, 1980), therefore, we are able to use similar analysis techniques to study the physical properties (electron densities and temperatures) and chemical abundances of the emitting gas of the star-forming regions (see e.g. Hägele et al., 2006) belonging to these low metallicity galaxies (Terlevich et al., 1991). BCDs present strong star formation easily identified through their intense Hα emission and narrow emission lines, low metallicity environments and complex star formation history. Due to these characteristics they are interesting objects to study metallicity effects in galaxies (Kunth & Östlin, 2000).
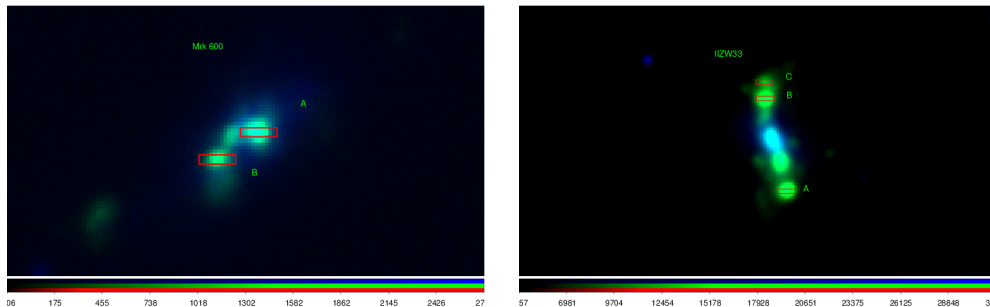
Figure 1.   Composite images of Mrk 600 (left panel) and IIZw 33 (right panel). Green and blue are Hα and R band, respectively, images acquired with the 1.8 telescope at Monte Palomar (images taken from NED). The echelle slits are overimposed.

Many BCDs that used to be considered compact objects, currently show a complex spatial structure thanks to the improvement and enlargement of telescopes and instruments (Hägele et al., 2011). For example, Haro 15, currently classified as a spiral galaxy, were included in BCDs catalogues (see discussion in Firpo et al., 2011; Hägele et al., 2012).

2.   Observations

Our data were acquired in 2005 and 2006, using the high resolution echelle spectrograph mounted at the Clay Magellan Telescope (6.5m) at Las Campanas Observatory (LCO), Chile. The spectrograph uses a dichroic to separate the light in 2 different spectral ranges. The 1x4 arcsec^2 slit was used with a blue and red spectral resolutions of R 28000 and R 22000, respectively. The blue and red spectral ranges were 3300-5100 Å and 4850-9300 Å, respectively. We used IRAF[1] routines in the usual manner to reduce the data. GD108 was used as standard star. We observed 5 star-forming knots: 2 belonging to Mrk 600 and 3 to IIZw 33. Each studied star-forming region was also divided in sub-components accordingly to the spatial components identified in its spatial profile (see the procedure description in §3). In total we have observations of 11 regions: 4 in Mrk 600 (2 components for each knot, A and B; see left panel of Fig. 1) and 7 for IIZw 33 (3 sub-components for Knot A, and 2 for knots B and C; see right panel of Figs. 1).

3.   Results

Spatial components

Analyzing the spatial profile around the Hβ emission line in the 2D echelle spectra we identified more than one different spatial components for each studied

---

[1]IRAF: the Image Reduction and Analysis Facility is distributed by the National Optical Astronomy Observatories, which is operated by the Association of Universities for Research in Astronomy, Inc. (AURA) under cooperative agreement with the National Science Foundation (NSF).
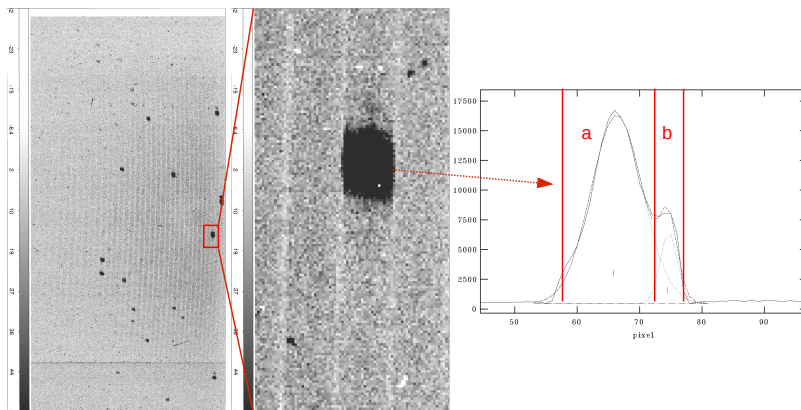
Figure 2. Left: 2D echelle spectrum corresponding to Mrk 600-B, showing different emission lines and orders. Middle: zoom of the 2D echelle spectrum around the Hβ emission line. Right: spatial profile at the position of the Hβ emission line. It can be seen two spatial components and the performed spatial-Gaussian fitting.

star-forming region (see an example of the 2D echelle spectra together with the Hβ spatial profile and the performed fitting in Fig. 2). We performed an extraction for each of the identified spatial components. We are able to perform the chemodynamical study for each of these spatial components.

Kinematical components

Following the methodology proposed, developped and used in Hägele et al. (2007, 2009, 2010, 2012, 2013); Firpo et al. (2010, 2011) we deconvolve the emission line profiles in different kinematical components. We performed the analysis of the strong emission lines detected in our regions using our own Python code based on the use of the LMFIT (Non-Linear Least-Squares Minimization and Curve-Fitting for Python) package. We proposed a model composed by a linear function and "n" Gaussians or normal distributions, to fit the local continuum and the emission-line profile, respectively. We started our analysis modeling the strongest emission-lines: Hα and [OIII]λ5007Å. Then, we used these kinematical results, line positions (velocities) and widths, as the initial approximations for the other emission-lines with similar ionization state. For [OI], [OII], [SII] and [NII] emission-lines we used the solution found for the Hα recombination line. While for HeI, [SIII], [NeIII], [ArIII] and [ArIV], we used the solution found for the [OIII]λ5007A emission-line. It must be noted that for the very weak temperature sensitive auroral emission-lines: [OIII] λ 4363Å, [OII] $\lambda\lambda$ 7319,7330Å, [NII] λ5755Å, [SIII] λ 6312Å, and [SII] λ 4068Å, we used the kinematical solution obtained for the strong emission-line of the same atomic ion since the kinematical solution must be the same (or very similar) and therefore we only varied their amplitudes (see a complete discussion about this point in Hägele et al. (2012). In Fig. 3 some examples of the results of the fittings to the emission-line profiles of Knot A of IIZw 33 are shown.
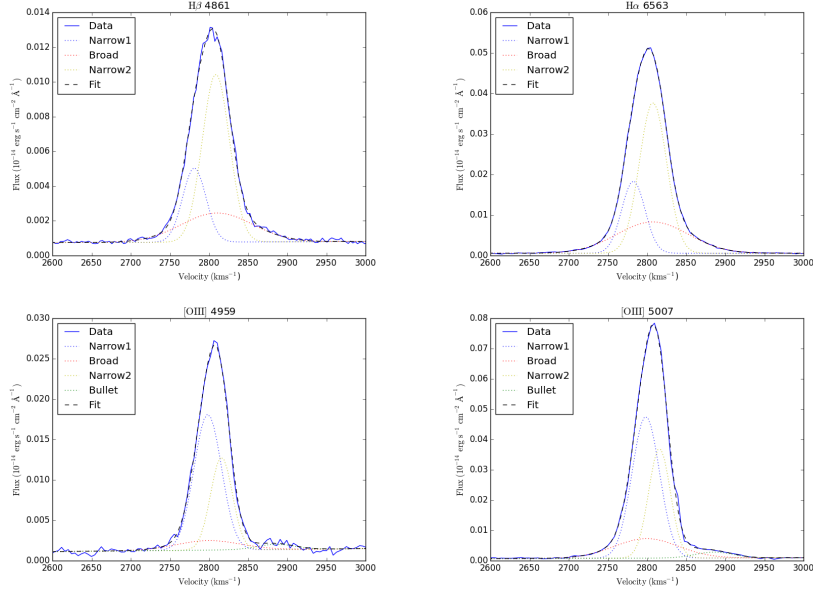
Figure 3.   Some results of the fittings performed to the emission-line profiles of Knot A of IIZw 33.

4.   Conclusions

We observed 11 star-forming knots belonging to 2 BCDs using high resolution echelle spectroscopy that will allow us to carry on a chemodynamical study of their physical conditions and chemical abundances. We used our own Python code base on the LMFIT package to perform the kinematical decomposition of the emission lines profiles. Our near future objectives are to derive for each kinematical component: (i) the reddening constant from the hydrogen recombination lines in all the regions; (ii) the electron density in the low excitation zone from the emission-line ratios of [SII]λ6717Å/λ6731Å and [OII]λ3727Å/λ3729Å; (iii) the electron temperatures Te ([OII]), Te ([OIII]), Te ([SII]), Te ([SIII]), and Te ([NII]) using the auroral emission lines present in the spectra of several of our regions and applying the direct method (see e.g. Hägele et al., 2008) or empirical relations and photo-ionization models (see e.g. Pérez-Montero & Díaz, 2005; Hägele et al., 2006); (iv) ionic abundances of He+, O+, O2+, S+, S2+, N+, Ne2+, Ar2+ and Ar3+; (v) the total chemical abundances of He, O, S, N, Ne and Ar; (vi) the ionization degree of the nebular gas from the η and η' parameters (Vílchez & Pagel, 1988); and (vii) the relationship between the luminosities and velocity dispersion: L vs. σ (see e.g. Bosch et al., 2002).
We also have observations of other 5 BCDs acquired using the echelle spectrograph mounted at the du Pont telescope at LCO, for which will continue our chemodynamical study.

References

Bosch G., Terlevich E., Terlevich R., 2002, *MNRAS*, **329**, 481

Firpo V., Bosch G., Hägele G. F., et al., 2011, *MNRAS*, **414**, 3288

Firpo V., Bosch G., Hägele G. F., Morrell N., 2010, *MNRAS*, **406**, 1094

French H. B., 1980, *ApJ*, **240**, 41

Hägele G. F., Díaz A. I., Cardaci M. V., et al., 2007, *MNRAS*, **378**, 163

Hägele G. F., Díaz A. I., Cardaci M. V., et al., 2009, *MNRAS*, **396**, 2295

Hägele G. F., Díaz A. I., Cardaci M. V., et al., 2010, *MNRAS*, **402**, 1005

Hägele G. F., Díaz A. I., Terlevich E., et al., 2008, *MNRAS*, **383**, 209

Hägele G. F., Díaz A. I., Terlevich R., et al., 2013, *MNRAS*, **432**, 810

Hägele G. F., Firpo V., Bosch G., et al., 2012, *MNRAS*, **422**, 3475

Hägele G. F., García-Benito R., Pérez-Montero E., et al., 2011, *MNRAS*, **414**, 272

Hägele G. F., Pérez-Montero E., Díaz A. I., et al., 2006, *MNRAS*, **372**, 293

Kunth D., Östlin G., 2000, *A&A Rev.*, **10**, 1

Pérez-Montero E., Díaz A. I., 2005, *MNRAS*, **361**, 1063

Sargent W. L. W., Searle L., 1970, *ApJL*, **162**, L155

Terlevich R., Melnick J., Masegosa J., et al., 1991, *A&AS*, **91**, 285

Vílchez J. M., Pagel B. E. J., 1988, *MNRAS*, **231**, 257